

# Invar effect of $\text{SrRuO}_3$ : Itinerant electron magnetism of Ru 4d electrons

T. Kiyama, K. Yoshimura, and K. Kosuge

*Division of Chemistry, Graduate School of Science, Kyoto University, Kyoto 606-01, Japan*

Y. Ikeda and Y. Bando

*Institute for Chemical Research, Kyoto University, Uji 611, Japan*

(Received 11 April 1996; revised manuscript received 14 May 1996)

We have investigated the temperature dependence of the unit-cell parameters and volume of  $\text{SrRuO}_3$  and  $\text{CaRuO}_3$  with the Debye-Scherrer x-ray-diffraction technique in the temperature range from 12 to 300 K. The volume of  $\text{SrRuO}_3$  is almost constant below the ferromagnetic transition temperature  $T_c$  of 160 K. This represents a discovery of the Invar effect in transition-metal oxides, which is known to exist in 3d transition-metal itinerant magnets, e.g., Fe-Ni alloys. This fact suggests that the Ru 4d electrons, which cause ferromagnetism, have a Fermi surface and form a conduction band similar to that in 3d Invar alloys. On the other hand, the temperature dependence of the volume of  $\text{CaRuO}_3$  can be well described by a Debye function, implying that thermal expansion is governed by phonons, and that magnetic ordering does not occur in this compound. [S0163-1829(96)52126-0]

Transition-metal oxides exhibit a variety of physical properties. The discovery of high- $T_c$  cuprate superconductors<sup>1</sup> has drawn much attention to transition-metal oxides, particularly to those which have perovskite-related structures. Among those, the series of ruthenium oxides has very interesting structural, electrical, and magnetic properties. The compound  $\text{Sr}_2\text{RuO}_4$  is isostructural to the high- $T_c$  superconductor  $\text{La}_{2-x}\text{M}_x\text{CuO}_4$  ( $M=\text{Ca}$ ,  $\text{Sr}$ , and  $\text{Ba}$ ) system, and recently was also found to be a superconductor with  $T_c \sim 0.9$  K.<sup>2</sup> Both  $\text{SrRuO}_3$  and  $\text{CaRuO}_3$  have an orthorhombically distorted perovskite structure [Fig. 1(b)] that is the same as  $\text{GdFeO}_3$ ; it is described as an orthoferrite structure, and belongs to the space group  $Pbnm$  at room temperature.<sup>3,4</sup> Both compounds show metallic conductivity.<sup>3</sup>  $\text{SrRuO}_3$  is a ferromagnet with  $T_c \sim 160$  K,<sup>5,6</sup> while  $\text{CaRuO}_3$  was not found to be magnetically ordered down to 4.2 K despite the large negative Weiss temperature, which ordinarily suggests antiferromagnetic interactions in this compound.<sup>7,8</sup> Kanbayasi tried to explain the difference in magnetic properties by assuming a ferromagnetic interaction for the Ru-Sr-Ru path and an antiferromagnetic one for the Ru-O-Ru path.<sup>9</sup> On the other hand, Fukunaga and Tsuda insisted that the more distorted structure of  $\text{CaRuO}_3$  changes the sign of the magnetic interaction.<sup>10</sup> The origin of determining the sign of the magnetic interaction in this system and the detailed electronic state of  $\text{CaRuO}_3$  have not been well understood. These compounds are very interesting from the viewpoint of itinerant-electron magnetism. To study these compounds further, x-ray diffraction at low temperatures was performed for  $\text{SrRuO}_3$  and  $\text{CaRuO}_3$  which found that  $\text{SrRuO}_3$  shows an Invar effect below  $T_c \sim 160$  K, while  $\text{CaRuO}_3$  showed no anomaly in the temperature range of  $12 < T < 300$  K.

Polycrystalline samples of  $\text{SrRuO}_3$  and  $\text{CaRuO}_3$  were synthesized by a conventional solid-state chemical reaction.  $\text{SrCO}_3$ ,  $\text{CaCO}_3$ , and Ru metals of 99.9% purity were mixed in a nominal composition, pressed into pellets, and heated in air at 1323 K for 24 h. The pellets were reground in an agate mortar, pressed, heated again at 1573 K for 24 h in air, and cooled down to room temperature at the rate of 1 K/min.

Powder x-ray diffraction patterns were taken from 12 to 300 K for both samples, using a Rigaku diffractometer and Cu  $K\alpha$  radiation. The peak positions were calibrated against Si as an internal standard, and the lattice parameters and other structural parameters were obtained with a least-squares fitting procedure. Magnetization of the polycrystalline  $\text{SrRuO}_3$  sample was measured by a quantum design superconducting quantum interference device magnetometer in the temperature range from 5 to 170 K under the magnetic field of  $0 < H < 4.5$  T. The value of spontaneous magnetization was determined by the conventional Arrott-plot method.

The change of the diffraction patterns of  $\text{SrRuO}_3$  with temperature in the measured temperature range indicates that  $\text{SrRuO}_3$  exhibits no structural transition and has the same crystal structure over the whole measured temperature range. The obtained structural parameters of  $\text{SrRuO}_3$  at 300 K are displayed in Table I with those of  $\text{CaRuO}_3$  at 290 K. Figures 2(a)–2(c) show the variations of the lattice parameters of the  $a$ ,  $b$ , and  $c$  axes of  $\text{SrRuO}_3$  with temperature, respectively. The variations of lattice parameters on temperature do not show discontinuous changes. It should be noted, however, that the variation of the lattice parameters of the  $b$  and  $c$  axes clearly indicates anomalies below 160 K. The length of the  $b$  and  $c$  axes are almost constant for  $12 < T < 160$  K, while the  $a$  axis shows a usual thermal expansion. These anomalies affect the temperature dependence of the volume of  $\text{SrRuO}_3$ . As shown in Fig. 2(d), the unit-cell volume of  $\text{SrRuO}_3$  is almost constant for  $T < 160$  K, and so  $\text{SrRuO}_3$  exhibits what is called the Invar effect. The solid line in Fig. 2(d) represents the result of fitting by the following function which expresses the contribution to thermal expansion by anharmonic parts of lattice vibration using the Debye model for the lattice specific heat:

$$V \cong V(T=0) + \int_0^T \frac{\gamma C_v}{B} dT \cong V(T=0) + \frac{9\gamma N k_B}{B} T \left( \frac{T}{\Theta_D} \right)^3 \int_0^{\Theta_D/T} \frac{x^3}{e^x - 1} dx, \quad (1)$$

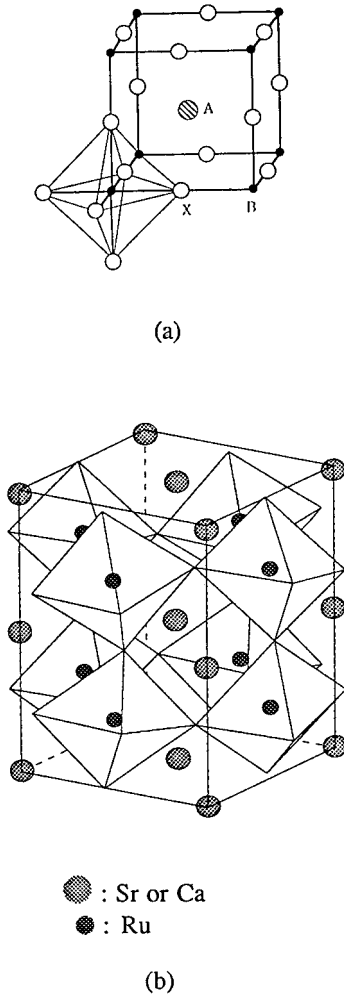


FIG. 1. Crystal structure of (a) cubic perovskite ( $\text{ABX}_3$ ) and (b) orthorhombically distorted perovskite. Ru atoms are coordinated octahedrally by oxygen atoms. (Oxygen atoms are omitted for brevity.)

where  $V(T=0)$ ,  $\Theta_D$ ,  $\gamma$ , and  $B$  represent the volume at 0 K, the Debye temperature, the Grüneisen parameter, and the bulk modulus, respectively.  $V(T=0)$ ,  $\Theta_D$ , and  $9\gamma Nk_B/B$  are the three fitting parameters and the parameters were determined through a least-squares fitting procedure in the temperature range of  $160 < T < 300$  K. The determined param-

TABLE I. Structural parameters for  $\text{SrRuO}_3$  and  $\text{CaRuO}_3$ .

Atom	Site	Occ.	$x$	$y$	$z$
$\text{SrRuO}_3$ $P_{nma}$ (No. 62) orthorhombic 300 K					
Ru	$4a$	1	0	0	0
Sr	$4c$	1	0.50(3)	1/4	0.99(8)
O(1)	$4c$	1	0.55(7)	1/4	0.50(6)
O(2)	$8d$	1	0.22(0)	0.03(7)	0.21(0)
$\text{CaRuO}_3$ $P_{nma}$ (No. 62) orthorhombic 290 K					
Ru	$4a$	1	0	0	0
Ca	$4c$	1	0.55(6)	1/4	0.01(5)
O(1)	$4c$	1	0.46(7)	1/4	0.59(1)
O(2)	$8d$	1	0.29(7)	0.05(3)	0.19(3)

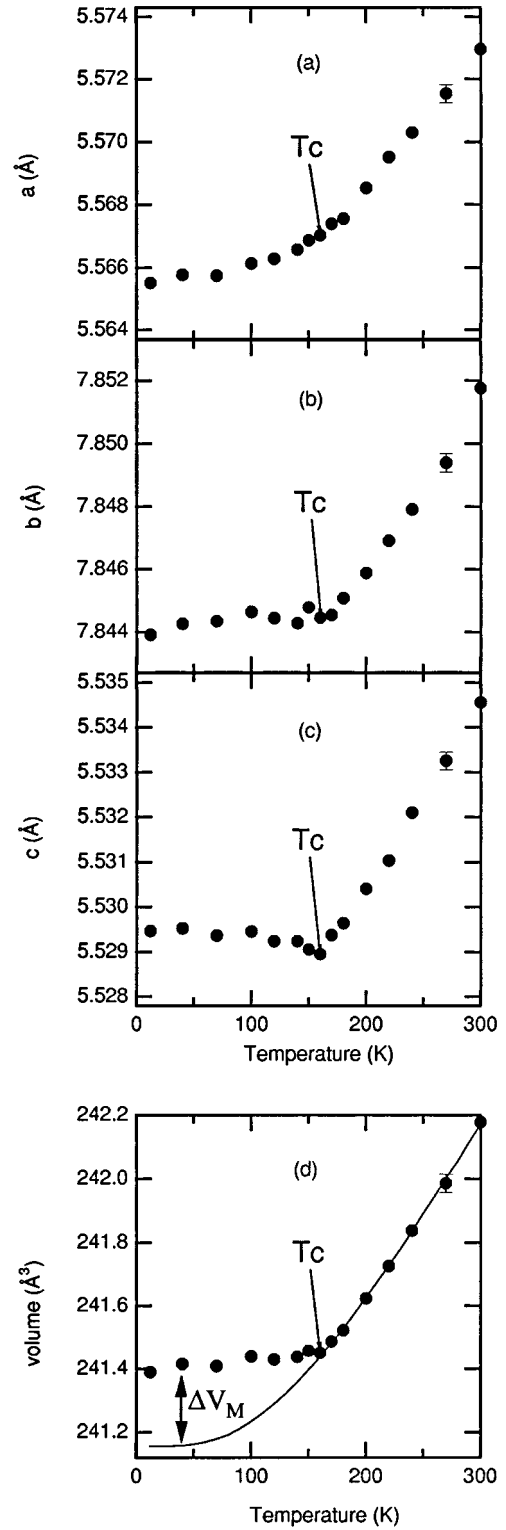


FIG. 2. Temperature variations of the unit-cell parameters (a)  $a$ , (b)  $b$ , and (c)  $c$  of  $\text{SrRuO}_3$ , respectively. Temperature dependence of the unit-cell volume of  $\text{SrRuO}_3$  is also shown in (d). The solid line represents the contribution of the phonon fitted by the Debye function with  $\Theta_D$  of 525.5 (K),  $V(T=0)$  of 240.9 ( $\text{\AA}^3$ ), and  $9\gamma Nk_B/B$  of 0.0281 ( $\text{\AA}^3/\text{K}$ ).

eters are shown in Table II. The obtained fitting line deviates very much from the observed values of the unit-cell volume under 160 K.

Figures 3(a)–3(c) also show the variations of the lattice

TABLE II. The parameters  $V(T=0 \text{ K})$ ,  $\Theta_D$ , and  $9\gamma Nk_B/B$  determined by a least-squares fitting using Debye function.

	$V(T=0 \text{ K}) (\text{\AA}^3)$	Debye temperature $\Theta_D (\text{K})$	$9\gamma Nk_B/B (\text{\AA}^3/\text{K})$
SrRuO <sub>3</sub>	240.9	525.5	0.0281
CaRuO <sub>3</sub>	226.3	542.0	0.0198

parameters of the  $a$ ,  $b$ , and  $c$  axes of CaRuO<sub>3</sub> with temperature, respectively. In the entire temperature range, CaRuO<sub>3</sub> has the same crystalline structure, and no discontinuity or anomaly was observed. Figure 3(d) shows the variation of the unit-cell volume of CaRuO<sub>3</sub> with temperature. The solid line represents the results of a similar fitting as mentioned above with SrRuO<sub>3</sub>. The obtained parameters are shown in Table II.

Unlike CaRuO<sub>3</sub>, the observed unit-cell volume of SrRuO<sub>3</sub> is much different from the result of fitting below 160 K. The obtained Debye temperatures of SrRuO<sub>3</sub> and CaRuO<sub>3</sub> are 526 and 542 K, respectively, and are almost equal. Then  $\Delta V_M$ , which was obtained by the difference between the measured volume and the calculated one [see Fig. 2(d)], is not thought to be caused by fitting procedure, but is thought to be an intrinsic property. It is suggested that the thermal expansion of SrRuO<sub>3</sub> is affected by another factor besides lattice vibration. The other factor is expected to originate from ferromagnetism, because the anomaly on volume occurs at the Curie temperature of SrRuO<sub>3</sub>. To elucidate the relation between the anomalous volume change and the ferromagnetism further, the following procedure has been tried:  $\Delta V_M$  and the  $M^2$  (=square of spontaneous magnetization) are plotted together against temperature in Fig. 4. Since the variations of these two sets of values show a good agreement, it is certainly believed that ferromagnetism of SrRuO<sub>3</sub> causes the anomaly of the thermal expansion.

In general, volume is affected by the magnitude of the magnetic moment through the magnetovolume effect according to the following equation:<sup>11</sup>

$$\omega_m = \sum_q (D_q/B) [\langle M_q^2 \rangle - \langle M_q^2 \rangle_0], \quad (2)$$

$$m_q = N_0^{-1} \int M(R) \exp(iqR) dR, \quad (3)$$

where  $\omega_m$  is the volume strain by the magnetovolume effect,  $B$  the bulk modulus,  $D_q$  the magnetovolume coupling constant depending upon  $q$ ,  $M(R)$  the spin density,  $M_q$  the Fourier  $q$  component of the spin density,  $N_0$  the number of unit cells in the crystal, and  $\langle \rangle_0$  means the average at  $T=0 \text{ K}$ . In itinerant electron magnetic substances, the magnitude of magnetic moment is generally reduced below  $T_c$  as temperature increases, while in magnetic insulators the magnitude of the magnetic moment is conserved regardless of temperature.<sup>12</sup> Therefore, itinerant electron magnetic substances have the negative contribution to thermal expansion below  $T_c$  because  $\langle M_q^2 \rangle$  generally reduces as temperature increases below  $T_c$ . Consequently it is expected that in SrRuO<sub>3</sub> the effect of the normal thermal expansion by lattice vibration and the reduction of magnetic moment compensate

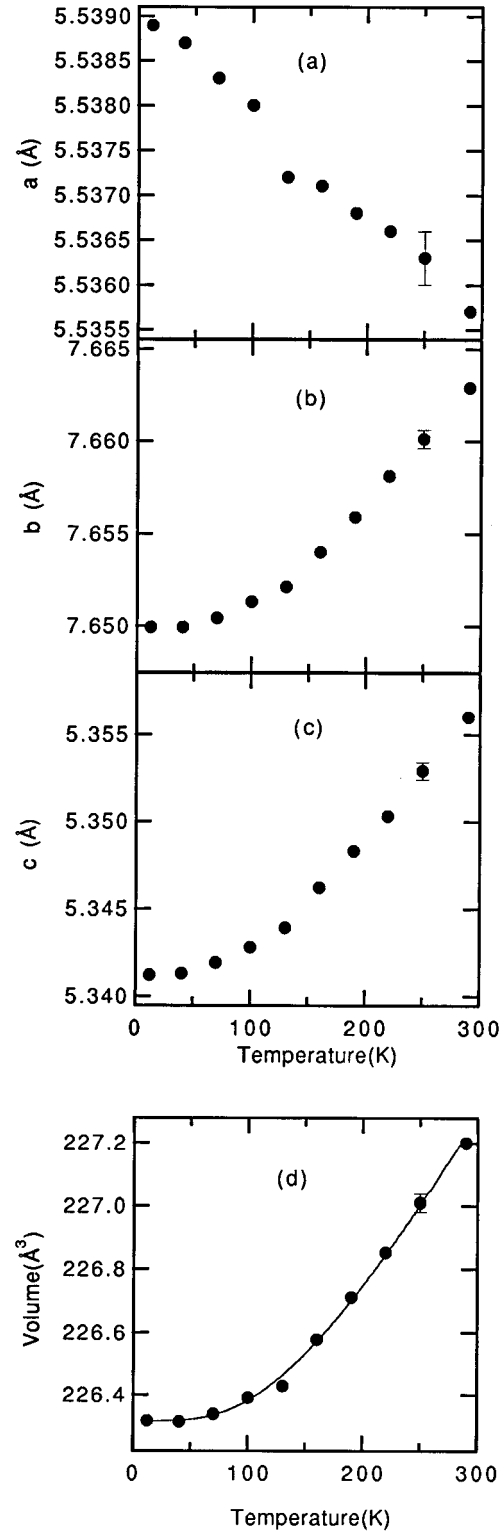


FIG. 3. Temperature variations of the unit-cell parameters (a)  $a$ , (b)  $b$ , and (c)  $c$  of CaRuO<sub>3</sub>, respectively. The temperature dependence of the unit-cell volume of CaRuO<sub>3</sub> is also shown in (d). The solid line represents the contribution of the phonon fitted by Debye function with  $\Theta_D$  of 542.0 (K),  $V(T=0 \text{ K})$  of 226.3 ( $\text{\AA}^3$ ), and  $9\gamma Nk_B/B$  of 0.0198 ( $\text{\AA}^3/\text{K}$ ).

each other and, as a result, the Invar effect appears as in the case of other 3d-Invar alloys. In other words, it is suggested that the 4d-band electrons in SrRuO<sub>3</sub> which cause ferromagnetism are itinerant and play a role in metallic conductivity.

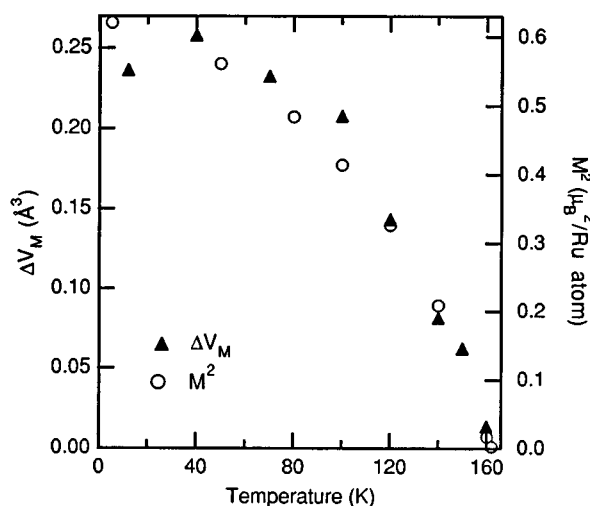


FIG. 4. Temperature dependence of spontaneous volume magnetostriction  $\Delta V_M$  (▲) and the square of the spontaneous magnetization  $M^2$  of SrRuO<sub>3</sub> (○).

As to CaRuO<sub>3</sub>, the fitting line well reproduces the observed variation of its unit-cell volume with temperature. It indicates that the contribution of the phonons principally rules the thermal expansion of this compound, and magnetic ordering of itinerant electrons as shown in SrRuO<sub>3</sub> is not expected to occur. This is consistent with previous reports.<sup>7,8</sup>

In Fig. 2, the  $b$  and  $c$  axes exhibit anomalies rather than the  $a$  axis in SrRuO<sub>3</sub>. Based on this fact, the magnetic easy axis is expected to be on the  $b$ - $c$  plane. Kanbayasi has studied the magnetization of a single crystal of SrRuO<sub>3</sub> and shown that this compound has a magnetic easy axis of  $\langle 110 \rangle$  when the unit cell is taken to be that of a pseudocubic perovskite structure [Fig. 1(a)].<sup>13</sup> Taking these two facts into consideration, the magnetic easy axis is expected to be the  $c$  axis of the orthorhombic unit cell, i.e.,  $\langle 001 \rangle$ .

In comparison with a typical Invar alloy Fe-Ni which has the volume strain  $\omega = \Delta V/V = 1 - 2 \times 10^{-2}$  ( $T=0$ ) and the square of spontaneous magnetization  $M^2 \sim 3.2 \mu_B^2/\text{atom}$ ,<sup>14,15</sup> SrRuO<sub>3</sub> has  $\omega \sim 1 \times 10^{-3}$  ( $T=0$ ) and  $M^2 \sim 0.6 \mu_B^2/\text{atom}$ , and then the ratio of  $\omega$  to  $M^2$  for Fe-Ni is 2–4 times larger than that of SrRuO<sub>3</sub>. It can be said that those values are very close, considering the differences of the  $3d$ - and  $4d$ -band widths or the number of magnetic atoms per unit volume between the two systems.

In conclusion, SrRuO<sub>3</sub> and CaRuO<sub>3</sub> do not indicate any structural transition or discontinuous changes of lattice parameters for  $12 < T < 300$  K. SrRuO<sub>3</sub> was first discovered to show the Invar effect below  $T_c \sim 160$  K in transition-metal oxides, and the  $4d$ -band electrons which induce ferromagnetism show itinerant electron character. On the other hand, CaRuO<sub>3</sub> exhibited no anomalies in the thermal expansion measurement, suggesting no magnetic order in this compound.

<sup>1</sup>J. G. Bednorz and K. A. Müller, Z. Phys. B **64**, 189 (1986).

<sup>2</sup>Y. Maeno, H. Hashimoto, K. Yoshida, S. Nishizaki, T. Fujita, J. G. Bednorz, and F. Lichtenberg, Nature **372**, 532 (1994).

<sup>3</sup>R. J. Bouchard and J. L. Gillson, Mater. Res. Bull. **7**, 873 (1972).

<sup>4</sup>S. Geller and E. A. Wood, Acta Crystallogr. **9**, 563 (1956).

<sup>5</sup>A. Callaghan, C. W. Moeller, and R. Ward, Inorg. Chem. **5**, 1572 (1966).

<sup>6</sup>J. M. Longo, P. M. Raccach, and J. B. Goodenough, J. Appl. Phys. **39**, 1327 (1968).

<sup>7</sup>J. B. Goodenough, Prog. Solid State Chem. **5**, 330 (1971).

<sup>8</sup>T. C. Gibb, R. Greatrex, N. N. Greenwood, and P. Kaspi,

J. Chem. Soc. Dalton Trans. **1973**, 1253 (1973).

<sup>9</sup>A. Kanbayasi, J. Phys. Soc. Jpn. **44**, 108 (1978).

<sup>10</sup>F. Fukunaga and N. Tsuda, J. Phys. Soc. Jpn. **63**, 3798 (1994).

<sup>11</sup>T. Moriya and K. Usami, Solid State Commun. **34**, 95 (1980).

<sup>12</sup>T. Moriya and A. Kawabata, J. Phys. Soc. Jpn. **34**, 639 (1973); **35**, 669 (1973).

<sup>13</sup>A. Kanbayasi, J. Phys. Soc. Jpn. **44**, 89 (1978).

<sup>14</sup>M. Hayase, M. Shiga, and Y. Nakamura, J. Phys. Soc. Jpn. **30**, 729 (1971).

<sup>15</sup>J. Crangle and G. C. Hallam, Proc. R. Soc. London Ser. A **272**, 119 (1963).